

A fully automated multi-spectral radioluminescence reading system for geochronometry and dosimetry

G. Erfurt^{a,1}, M.R. Krbetschek^a, V.J. Bortolot^b and F. Preusser^{c,d}

^a*Sächsische Akademie der Wissenschaften zu Leipzig, Quaternary Geochronology Section, TU Bergakademie Freiberg, Institute of Applied Physics, Bernhard-von-Cotta-Str. 4, 09596 Freiberg, Germany*

^b*Daybreak Nuclear and Medical Systems Inc., 50 Denison Drive, Guilford, CT 06437, USA*

^c*Geographisches Institut, Universität zu Köln, Albertus-Magnus-Platz, 50923 Köln, Germany*

^d*Institut für Geologie, Universität Bern, Baltzerstr. 1-3, CH-3012 Bern, Switzerland*

Abstract

Following the recent development of a new solid state luminescence dating technique for geochronometry that uses the infrared radiofluorescence (IR-RF) at 1.43 eV (865 nm) of potassium feldspars, an automated radioluminescence (RL) measurement instrument was designed and built. The instrument is based on a commercial Daybreak 1100 automated TL reader system, widely used in thermoluminescence (TL) dating. It was re-designed and highly modified to adapt it to the physical and methodological needs of the IR-RF dating technique and other RL dosimetry applications. This new system holds up to 10 samples, has an integrated bleaching and irradiation unit, and measures the radiofluorescence (RF) (excitation using 10^{137}Cs sources, each 5 MBq activity) as well as phosphorescence effects. All technical requirements for the measurement of optically excited luminescence were implemented in order to investigate the defect structure of luminescent materials. Because of the broad wavelength range and the high sensitivity of the photomultiplier detector used, the system is suitable for a great many luminescent materials, natural and synthetic. This paper summarises the technical features and performance criteria of the system. Furthermore, a calibration method and the dosimetric concepts, using the blue RF emission of $\text{Al}_2\text{O}_3:\text{C}$ at 415 nm for the β source dose rate estimation with low calibration errors is described in detail. Finally, examples of IR-RF dating results on Quaternary sediments as well as of other RF measurements and their physical interpretation using different RF emissions are presented.

Key words: radioluminescence, radiofluorescence, IR-RF, feldspar, Al₂O₃:C, luminescence dosimetry, luminescence dating, luminescence reader

1 Introduction

Radiofluorescence (RF) is a well known luminescence phenomenon, which arises from prompt radiative recombinations of charges after excitation by ionising radiation in crystalline semiconductors and insulators. Historically, the RF of ZnS helped raise Rutherford to the scientific Pantheon when he used this phenomenon to determine the scattering of α particles in a gold foil to prove the existence of atomic structure (1). This prompt fluorescence during irradiation with ionising radiation has also been used to distinguish the quality of diamonds by measuring the RF produced by their impurities (2). It may also be applicable to detection of unwanted effects on optical devices in radioactive environments (3) as well as in the clarification of defect characteristics in crystalline solids (4; 5). Luminescence dosimetry, and the luminescence dating procedures derived from it, use wide bandgap insulators. These are characterised by thermally or optically sensitive electronic levels in the bandgap which act as trapping and recombination sites for charge carriers stable—ideally—over the period studied (age span or time of storage). During interaction with ionising radiation, electrons and holes are excited in different ways and this may lead to an increasing population in trapping and recombination centers, respectively. Thermoluminescence (TL) and optically stimulated luminescence (OSL) protocols—which are basically radiophosphorescence (RP) processes—measure the relative density of electrons by secondarily excited (thermally or optically) radiative transitions of charges from traps into recombination centers (6). In contradistinction, the radiofluorescence measures the relative densities of electrons and holes on primary effects and, due to the continuous excitation by ionising radiation, in a transient equilibrium. The physical processes occurring while the RF is measured are straightforwardly similar to those which take place during the irradiation of the crystals in radiation fields of dosimetric interest.

A method of an UV-RF measurement on quartz extracted from bricks was described for retrospective dosimetry of the Chernobyl accident (7). Other authors investigated the spectral and dosimetric RF behaviour on LiF:Mg,Ti (8) and on Al₂O₃:C (9). Apart from applications of the radiofluorescence mentioned above, there have been recent developments in the field of luminescence

¹ Corresponding author: G. Erfurt; Phone: +49 3731 39 2163; Fax: +49 3731 39 4004; Email address: gerfurt@physik.tu-freiberg.de

geochronometry. The usefulness of the dosimetric application of radiofluorescence in dielectric media was affirmed when an infrared emission from potassic feldspar at 865 nm (1.43 eV) was carefully studied; its dosimetric behavior is suitable in Quaternary sediments for the age determination of the last light exposure, with an age range of up to 250 ka (derived from the mean IR-RF saturation dose of 800 Gy (10; 11; 12)). Comparing common luminescence dating techniques (13; 14; 15), the dosimetric information depends directly on the stability of the trapping states and not directly on the stability of the recombination centers. In addition, with the measurement of the prompt luminescence during the interaction of the feldspar grains with irradiation, one receives direct information about the electron population in the traps. The infrared emission in potassium feldspar at 865 nm represents the transition of electrons from the conduction band via the excited state of the trap in its ground state, which was fundamentally concluded from its opposite dose characteristics (single exponential decay) comparing TL and OSL and other RF techniques. Current investigations into the IR-RF of K-feldspar propose that its dose characteristics may depend on the complex kinetics of all radiative and non-radiative charge transitions within the minerals and on a second electron transition (emission at 910 nm) into the ground level of the 1.43 eV trap, but from another excited state in the same, luminescence creating ion (16).

There is a paper on an automated instrument which has measured radiofluorescence, but only in the UV-VIS wavelength range (17). Because of our new instrument's measurement flexibility, the first dating results (11), and the fact that a reliable luminescence dating technique for older clastic sediments (older than 150 ka) does not exist, the fully automated radioluminescence reading instrument we describe here has distinct advantages for geochronometry as well as for dosimetry and luminescence research. This instrument is able to detect luminescence light from 160 nm to 920 nm. Furthermore, we report in this present paper on a highly precise β source calibration protocol using the blue RF emission at 415 nm of $\text{Al}_2\text{O}_3:\text{C}$, on dating results of Quaternary sediments and other possible RF measurements using the new RL reader.

2 Experimental

2.1 General notes

Radiofluorescence spectra of samples GOS4, HURL1, KOE10a, K6, K7 and K9 were measured using a highly precise CCD-based luminescence spectrometer described elsewhere (10; 18). RF spectra were excited by an ^{137}Cs source with an activity of 3.5 MBq.

In the present paper, IR-OSL measurements on K-feldspar samples GOS4 and HURL1 were carried out using a Risø TL-DA-12 reader (19). 40 aliquots were normalised by short exposure (0.1 s) to IR-diodes and irradiated using a ^{60}Co γ source ($\approx 7 \text{ Gy min}^{-1}$). Six dose groups five aliquots each have been used for constructing a dose response curve. Prior to measurements the sample was stored for more than four weeks at room temperature and pre-heated at 160°C for 16 h to remove unstable components of the signal. IR-OSL was recorded during a 60 s shine down of IR-diodes applying a detection filter set with a peak transmission at $\approx 410 \text{ nm}$ (Schott BG 39, Schott GG40, Corning 7-59). The integral 50-60 s was substrated from the rest of the shine down curve as late-light.

Following investigations of Krbetschek et al. (20), K-feldspar samples for spectral and dosimetric studies were bleached 30 minutes.

γ irradiation for the calibration of the β sources was carried out on a ^{60}Co source at STEP Sensortechnik Pockau GmbH/Germany. Samples were irradiated by a dose rate of about 500 mGy h^{-1} with an error of 2%.

2.2 *The radioluminescence reader*

The RL system presented in this paper is based on a commercial Daybreak 1100 TL reader (without its usual lid, vacuum plumbing, or luminescence light detection (21)) and re-designed expressly for RL measurements. Bearing in mind the physics as well as the methodology of the IR-RF dating technique (16; 20; 22) and requirements for the measurement of RL in general, the following technical needs were considered:

- High quantity of samples for routine dating tasks
- Broad band luminescence detector for all emissions in the UV to near IR
- Fast automatic optical filter exchange
- Bleaching facility within the instrument
- Broad band OSL excitation for dating and defect spectroscopy
- Software solution for full automation
- Possibilities for extension to new techniques deriving from current investigations

The RL reader is schematically presented in figure 1.

The sample turning system consists of an upper and a lower platter, 0.5 mm apart, connected through a coaxial shaft to the central gear motor, with a mechanism for changing the phase of the two platters, so that the sample irradiation may be 'switched' on and off. The lower platter holds ten ^{137}Cs sources (V.G. Khlopin Radium Institute St. Petersburg, Russia), which were chosen as

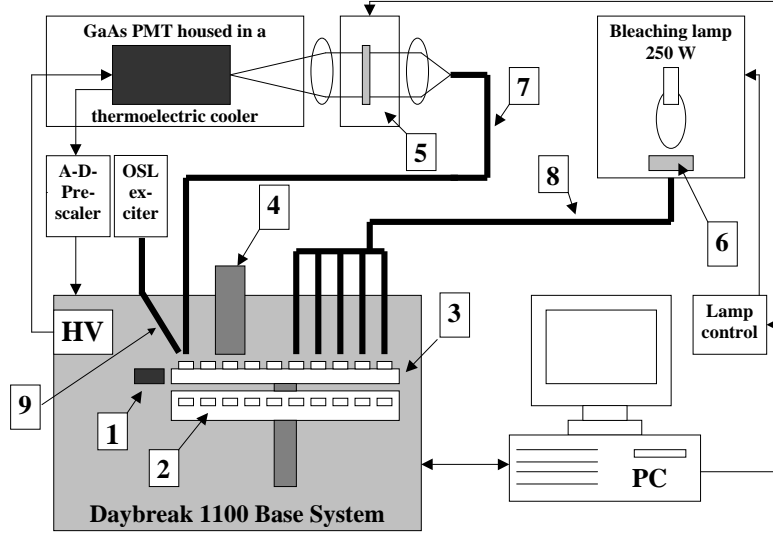


Fig. 1. Scheme of the RL automated system: 1-heating plate, 2-source platter holding 10 ^{137}Cs sources, 3-sample platter for 10 samples, 4-inlet tube for samples, 5-automated filter wheel (4 positions), 6-IR absorbing filter= Schott KG3, 7-signal optical fiber cable, 8-bleaching optical fiber cable (1 to 5), 9-optical fiber cable for optical excitation

RL excitation and irradiation sources (single activity of 5 MBq (05/20/2000) and an active area of 8 mm). Apart from the half-life (30.2 y), β spectrum ($E_{\text{end}}= 513.97$ keV (94.4%), $E_{\text{end}}=892.22$ keV (0.000588%), $E_{\text{end}}=1175,63$ (5.62%)) and conversion electrons (624 keV, 656 keV), the sources were chosen according to German radiation protection regulations. The disadvantage of this radionuclide is the γ radiation at 662 keV, which has to be shielded. It should be mentioned that the γ part from the sources does not influence the RF signal of the samples adversely. Because of the mono-layer of the dosimeter grains with a thickness of $\approx 100..150 \mu\text{m}$, the linear energy transfer (LET) to the samples is too small to build up a measurable γ dose. A reproducible mono-layer of the samples can be prepared using adhesive mylar foil strips which are fixed on special sample plates. This also prevents the attenuation of the transmitting β particle and electron beam.

The upper platter holds the sample plates. This double platter system is turned together by the common, central shaft, but a second gear motor linking an eccentric cam makes possible the relative movement of the two platters. This arrangement allows the samples to be irradiated or to be shielded from the sources. The movement from one position to another is quite precise and the radiation geometry is not changed.

The luminescence from the excited sample is collected by a fiber optic cable which is mounted to a filter wheel (sample end: no optics, filter wheel end:

f/2 optics). This computer-controlled filter wheel (Oriel) offers five filter positions. One position is reserved for a shutter for measurement of dark count rate; the others can be chosen according to the particular task. For measuring the IR luminescence of feldspar, custom interference (Andover 200FC35) or fluorescence (Andover HQ865/20M) filters, both centered at 865 nm, are installed. A small bandwidth of about 10 to 15 nm FWHM is important, because of an interfering peak at 700 nm typical for all feldspars, whose intensity increases with delivered dose; its gaussian shape overlaps the decreasing IR-RF emission (20; 22). The automated filter wheel makes it possible to measure several different emission bands at once. For the detector, a Hamamatsu GaAs:Cs photomultiplier (PMT) type R943-02 was chosen (23), and housed in a thermoelectric cooler to minimize dark count rates. This PMT has a spectral response range from 160 to 930 nm. The peak wavelength range from 300 to 800 nm shows a quantum efficiency of 10%. At 865 nm, the quantum efficiency is still about 5%. For the bleaching performance a one-to-five fiber optic was connected to an Osram 250 W metal halide lamp (HTI series) with a color temperature of 5600 K. Its spectrum is close to the solar radiation conditions in middle Europe at the lower troposphere. The lamp seems to be a good alternative to expensive solar light radiators, and the infrared part of the emitted spectrum is absorbed by a Schott KG3 short pass filter with an IR cut-off wavelength of 900 nm. Five of the ten samples are bleached at one time with a radiative power input of $P_{\text{rad}} \approx 100 \text{ mW cm}^{-2}$ each.

Another measurement configuration employs an optical excitation unit for defect spectroscopy or for OSL measurements. This device consists simply of an optical fiber cable illuminating the sample plate in measurement position; the other end of the fiber can be connected to various light sources (automated, pulsed, etc.). The major difficulty with this arrangement is the suppression of undesired excitation light that might be transmitted to the detector. A forthcoming solution uses new narrowband fluorescence filters with nearly 100% out-of-band blocking.

The thermoluminescence nichrome heater of the Daybreak 1100 system can be used for pulse annealing or other thermal treatments of the samples. In contradistinction to the apparatus presented by Poolton et al. (17), the radiofluorescence can not be measured at elevated temperatures.

A control program for complete automation of all devices and processes was designed using the Keithley TestPoint software development kit.

2.3 *Radiofluorescence measurement performance*

The automated filter wheel and the UV-IR sensitive PMT make it possible to investigate all common luminescent materials (24). Any desired number of dose points may be read, until energy saturation of the dosimeters is reached (for IR-RF commonly a few hundred points). The more dose points measured, the higher the data density there is describing the dose characteristics. Modeling of luminescence kinetics can be controlled by the precision of the parameter estimation of the dose curve fit functions. The mathematical interpretation of the RF dose curves of various materials can be found elsewhere (12; 16; 24). For age estimation using the IR-RF of K-feldspar, a single-aliquot regenerative-dose dating protocol (IRSAR) is applied (22). Before any RF measurement is taken, the overall sensitivity of the system and the dark current of the photomultiplier are measured; the latter is automatically subtracted from the mean value of the luminescence signal.

Cross-talk problems are negligible; neither the dose delivered to adjacent sample positions, nor any leakage if the sources are moved from beneath the samples are significant. The dose delivered to adjacent sample positions is considered in the source calibration (see section 3); if the sources are removed, the dose rate is negligible. In a test on K-feldspar, there was no measurable dose. Since the bleaching of only a single sample at one time is not required, the spill-over of bleaching light is not a matter of particular interest.

In future work more attention should be paid to the optical excitation unit when investigating defect structures of minerals and synthetic luminophors.

2.4 *Sample description and preparation*

2.4.1 *Geological settings*

K-feldspar sample GOS4 was taken from overbank deposits exposed in a gravel pit near Gossau, Switzerland. The age of a peat layer just below the sampled horizon has been dated by radiocarbon to ≈ 32 cal. ka (25) and to 34.7 ± 4.0 ka by U/Th (26). For the overbank deposits, several IR-OSL ages of about 29..30 ka have been determined using the multiple-aliquot additive-dose (MAA) technique on polymineral fine-grain and K-rich feldspars, respectively (27; 28).

K-feldspar grains extracted from sample HURL1 originate from a sandy layer associated with sinter deposits along the river Lech, southern Germany. The sediment is interpreted to be of last interglacial age ($\approx 115..130$ ka, according to marine isotope stratigraphy (29) based on mollusc fauna (30) and palynology (31)). The sinter was dated by the U/Th method to 120.3 ± 5.8 ka (31). For the

sandy layer, an IR-OSL age of 134.8 ± 11.6 ka was determined using a MAA approach described in section 2.1.

Sample KOE10A is a K-feldspar sample extracted from a fluvial deposit near Bad Kösen/central Germany. It belongs to the Saalian complex, the most cold period between the Eemian and the Holsteinian interglacial stage. According geological information and luminescence data from central Germany, its age range can be assumed to be between 150..220 ka.

Sample SHO was taken in an open lignite pit mine in Schöningen/northern Germany close to the excavation site of the world oldest Paleolithic hunting weapons (description see Thieme (32)). This K-feldspar sample is believed to be older than 300 ka, but in this study it was chosen used for dosimetric measurements only.

Samples K6, K7 and K9 are rock-forming K-feldspars from the Mineralogical and Petrographical Collection at the Freiberg University of Mining and Technology. XDA analysis and other detailed mineralogical investigations were carried-out by Dütsch (33).

2.4.2 Sample preparation

The $\text{Al}_2\text{O}_3:\text{C}$ dosimeters (Landauer, USA) of the grain size of 90..106 μm were annealed at 900°C for 15 minutes before being used for intercalibration with a γ source of known dose rate.

The rock-forming K-feldspar samples K6, K7 and K9 and their preparation are described by Dütsch (33). Sample GOS4, HURL1, KOE10A and SHO were treated with hydrochloric acid and hydrogen peroxide to remove carbonates and organic matter before separation of grains of potassium feldspar using heavy liquids with a density of 2.58 g cm^{-3} . KOE10A and SHO underwent additional feldspar flotation before density separation. Sediment dose rates were calculated from specific activity estimation using γ spectrometry data of the samples. The total dose rates (including the cosmic ray contribution) of samples GOS4, HURL1 and KOE10A were $2364 \pm 166 \mu\text{Gy a}^{-1}$, $2349 \pm 189 \mu\text{Gy a}^{-1}$ and $3340 \pm 300 \mu\text{Gy a}^{-1}$, respectively.

3 Calibration of β sources

3.1 Physical aspects of β dosimetry for luminescence dating

The calibration of β sources in general and especially of those applied to luminescence dating has been a serious problem; different physical facts have to be considered in order to yield results both precise and accurate. In luminescence dating the accumulated dose D_e („palaeodose“) of a sample is estimated using equation 1:

$$\begin{aligned} D_e &= \int_0^t \sum \dot{D}(t) dt \\ &= \int_0^t [\dot{D}_\alpha(t) + \dot{D}_\beta(t) + \dot{D}_\gamma(t) + \dot{D}_i(t) + \dot{D}_k(t)] dt, \end{aligned} \quad (1)$$

where $\sum \dot{D}(t) = \dot{D}_\alpha(t) + \dot{D}_\beta(t) + \dot{D}_\gamma(t) + \dot{D}_i(t) + \dot{D}_k(t)$ is the natural dose rate with its contributions from α , β , γ radiation in the surrounding of the sample and internal and cosmic parts (see (15)). This natural dose rate is assumed to be time-independent. With this simplification, the age t of the sample can be determined by the quotient

$$t = \frac{D_e}{\sum \dot{D}}. \quad (2)$$

The dose rate $\sum \dot{D}$ in natural environments is estimated by measuring the radionuclides within both the sample and its environment. With those specific radionuclide constituents measured it is possible to calculate the dose rate based on fundamental material parameters, such as density, effective Z , stopping powers and energy attenuation parameters, self absorption effects, water content of the sediment and so on. The palaeodose D_e estimation using luminescence techniques is a completely different procedure and its accuracy depends primarily on the accuracy of the dose rate calibration of the applied laboratory β sources. This accuracy and precision depend on the observed influence of intrinsic and extrinsic defects. Theoretically, this implies that the calibration of the β sources has to be carried out for each individual quartz or feldspar sample since the differing defect inventory might lead to a different luminescence-dose response. The luminescence intensity is proportional to the absorbed dose, but for natural dosimeters the functional behaviour is not well known, due to varying physical and chemical conditions during mineral formation (e.g. for quartz see (34)). Unlike the synthetic luminophors

applied to personal luminescence dosimetry, we have incomplete knowledge of the energy dependence of the luminescence sensitivity for natural dosimeters like feldspar and quartz. For this reason and because of other complex effects which accompany the dose-generating energy transfer of β particles and electrons in matter (scattering processes, etc.), a precise luminescence calibration of β sources needs a well known dosimeter material with high sensitivity and (preferably) a known dependence of the luminescence sensitivity vs. radiation energy, as well as a linear dependence of luminescence response vs. applied dose. For the calibration of β sources used in the present instrument, the radiofluorescence characteristics of a calibration material should be suitable for this specific dosimetric application. This is not a new idea, since in the early 70's the calibration of β sources applied to luminescence dating using CaF_2 probe dosimeters had already been described (35). The main problem using CaF_2 dosimeters is the effective Z of 16.6, quite far from the effective Z of quartz (≈ 10.0) and feldspar (≈ 10.6).

Even those general dosimetric problems combined with less known material characteristics of natural dosimeters are known, the calibration of β sources used in luminescence dating is commonly carried out applying TL or OSL protocols to natural quartz samples, which were intercalibrated against a known γ source (e.g. described by Göksu et al. (36)). However, the radiofluorescence qualities of quartz do not enable this mineral for the use as reference dosimeter for RF source calibration. Therefore an attempt to use feldspar was undertaken, but a high scattering of the calibration data has been observed (37).

3.2 Radiofluorescence β dosimetry using $\text{Al}_2\text{O}_3:\text{C}$ (TLD 500)

Following the results of an earlier study (24) on its radiofluorescence characteristics, the TL/OSL anion-defective dosimeter material $\text{Al}_2\text{O}_3:\text{C}$ (TLD 500) was especially chosen for the calibration of β sources installed in the RL instrument. Radiofluorescence dosimetry using the blue emission (415 nm) of $\text{Al}_2\text{O}_3:\text{C}$ (38) was described recently (39; 40). The luminescence sensitivity is 50 times higher than that of $\text{LiF}:\text{Mg},\text{Ti}$ (TLD100) (38). The TL signal is stable over a period of two years (41), and the stability of the blue RF signal was also proven (39). This high luminescence sensitivity vs. radiation energy is well known (42), as well as the TL, OSL and RF dose characteristics of the dosimeter (39; 42; 43). Beside these characteristics, $\text{Al}_2\text{O}_3:\text{C}$ shows only a negligible fraction of defects which create shallow energy levels, an important factor for radiofluorescence dosimetry. The RF signal is therefore not influenced by charge transitions into shallow traps or recombination centers and depends only on transitions into stable centers. The bright blue radiofluorescence of $\text{Al}_2\text{O}_3:\text{C}$ (about 25 times higher than the IR-RF emission of feldspar) leads to good photon counting statistics. The energy dependent sensitivity of

the luminescence response of $\text{Al}_2\text{O}_3:\text{C}$ was investigated (38; 42) and shows a constant response from 0.2 MeV to 1.0 MeV. However, in the lower energy region up to 0.2 MeV, the luminescence sensitivity of the material is characterised by a dependence on the energy over up to factor 3. With regard to the mean β energy (≈ 520 keV) and the energies of the internal conversion electrons (624 keV and 656 keV) of ^{137}Cs , a correction is not particularly necessary at this time, but should be examined in future studies for the sake of completeness. Comparing the sensitivities of luminescence dosimetry and γ spectrometry methods for the measurement of a dose rate (44), the highly sensitive material $\text{Al}_2\text{O}_3:\text{C}$ seems to be the ideal choice for yielding high precision and accuracy, also as regards equation 2. Furthermore, the effective $Z=10.2$ is equal to that of quartz and feldspar.

3.3 Theory of β dosimetry

The dose D_m , delivered by collision interactions of monoenergetic electrons with matter is expressed by equation 3,

$$D_m = \Phi(E_1) \cdot (S/\rho)_m^{col}(E_1) \quad (3)$$

where $\Phi(E_1)$ is the fluence of the monoenergetic electrons and $(S/\rho)_m^{col}(E_1)$ is the collision contribution of the mass stopping power at the energy E_1 . The commonly used irradiation sources used in luminescence dating ($^{90}\text{Sr}/^{90}\text{Y}$ and ^{137}Cs) emit β particles (and/or conversion electrons (IC)) with different energies and therefore, the spectral fluence distribution must be considered as written in equation 4.

$$D_m = \int_0^{E_{max}} \Phi(E) \cdot (S/\rho)_m^{col}(E) \cdot dE \quad (4)$$

If the mean mass stopping power $(\bar{S}/\rho)_m$ (collision and bremsstrahlung) is known, the dose D_m can be simplified as

$$D_m = \Phi \cdot (\bar{S}/\rho)_m \quad (5)$$

where Φ is the total particle fluence. If a probe substitutes for a sample (e.g. feldspar substituted by $\text{Al}_2\text{O}_3:\text{C}$), and its mean mass stopping power $(\bar{S}/\rho)_p$ is different from that of the sample $(\bar{S}/\rho)_m$, the probe should modify neither the number and energy nor the direction of the electrons which cross the probe (Bragg-Gray conditions (45; 46; 47)). If this condition is fulfilled, the dosimetry is independent of the fluence. Therefore, the relation between the

mass stopping powers of the probe and the substituted material can be used. Taking this quotient into account, the dose given to the sample (D_m) can be calculated from the dose delivered to the probe (D_p) using equation 6.

$$D_m = \frac{(\bar{S}/\rho)_m}{(\bar{S}/\rho)_p} \cdot D_p \quad (6)$$

3.4 Practical notes

An intercalibration method using Al_2O_3 requires the resulting dose rates to be converted to the correlative feldspar values, following the theory reported in section 3.3. One limitation is the energy distribution of the β spectrum. Because it is not trivial to calculate the dose for the given spectrum, we use the mass stopping power at the mean energy of the β spectrum. This should not lead to serious problems because of the similarity of the mass stopping powers for Al_2O_3 and feldspar, calculated using data from ICRU report no.37 (48) (figure 2).

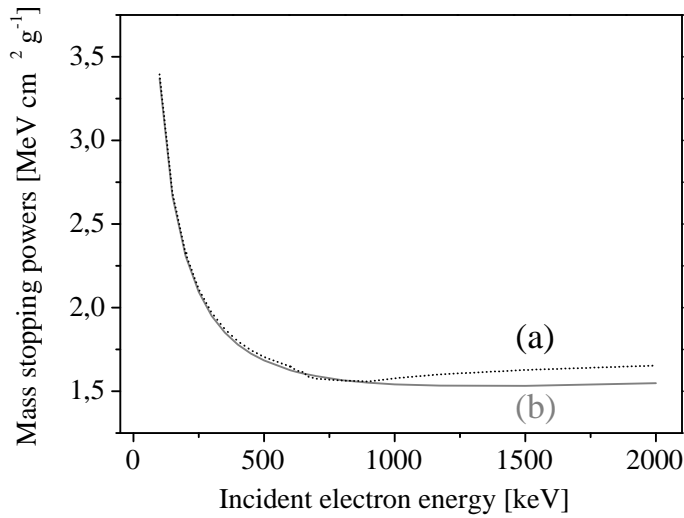


Fig. 2. Total mass stopping powers calculated using data from ICRU report no.37 (48). (a) potassium feldspar $\text{K}[\text{AlSi}_3\text{O}_8]$ and (b) aluminium oxide Al_2O_3

Since the β sources are calibrated against a defined γ source, the different mass energy attenuation factors of the medium in which the γ source is calibrated (standard medium is air) and $\text{Al}_2\text{O}_3:\text{C}$ have also to be taken into account. For ionising photons, the general idea is the same as for β particles and electrons, and the γ dose delivered to $\text{Al}_2\text{O}_3:\text{C}$ can be derived (49).

Very important is the choice of a container material ('build-up') due to the concept of charged particle equilibrium (CPE) in the $\text{Al}_2\text{O}_3:\text{C}$ dosimeters. To fulfill this concept, $\text{Al}_2\text{O}_3:\text{C}$ grains must ideally be irradiated in a 4π geometry and packed in a container made of Al_2O_3 . Practically, materials with a density of $\approx 4 \text{ g cm}^{-3}$ can be used (e.g. sintered corundum). The thickness of the container material must be larger than the maximum range of the secondary charged particles.

The $\text{Al}_2\text{O}_3:\text{C}$ samples were irradiated in a ^{60}Co γ field (as an air dose equivalent). The measurement inaccuracy of these irradiations is about 2 %. The applied γ dose was 19.59 Gy in air. Note that the mass density (expressed by sample thickness or grain size) of the material to be used as probe dosimeter (the mass density includes integral depth dose distribution) must also be considered, in comparison to the material under calibration, since the mass stopping powers are density normalised quantities. E.g. if the grain size for feldspar coarse grain dating is about $150 \mu\text{m}$ ($\rho=2.56 \text{ g cm}^{-3}$), the grain size for $\text{Al}_2\text{O}_3:\text{C}$ ($\rho=3.97 \text{ g cm}^{-3}$) is subsequently $100 \mu\text{m}$ —which fits well to the grain size of $90..106 \mu\text{m}$ used in the present work. A typical dose characteristic of the blue RF of $\text{Al}_2\text{O}_3:\text{C}$ at 3.00 eV (415 nm) is shown in figure 3, together with an example of the calibration.

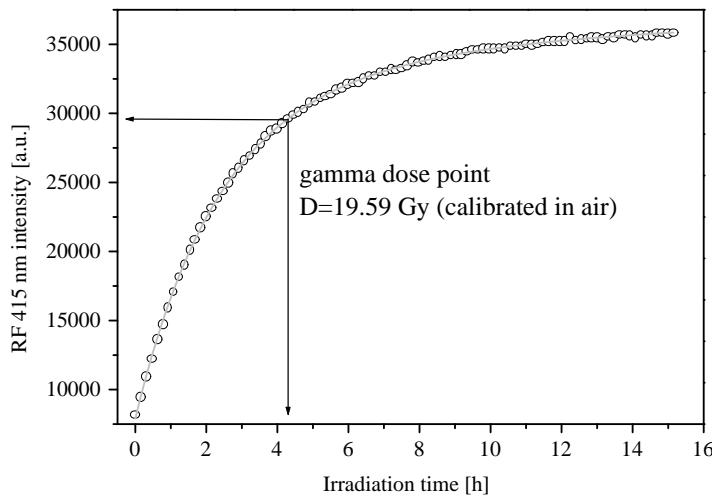


Fig. 3. Dose characteristic of the 415 nm peak of $\text{Al}_2\text{O}_3:\text{C}$. The data (open circles) were fitted to an exponential function (grey line). The indicated intercalibration point at 19.59 Gy illustrates the β calibration method after Erfurt et al. (39)

For these measurements, an 415 nm interference filter was placed in the filter wheel. After measuring the RF at the γ dose point, the samples were bleached in accordance with the bleaching behaviour of $\text{Al}_2\text{O}_3:\text{C}$ (50). The dosimetric

luminescence sensitivity of $\text{Al}_2\text{O}_3:\text{C}$ to UV-B light in the wavelength region 280 nm to 320 nm described by Colyott et al. (51) has not to be taken into account, because the bleaching lamp of our instrument does emit light below 320 nm only to a very small extend. Using the fit results applying the exponential function

$$\Phi(D) = \Phi_0 + \sum_i \Delta\Phi_i \cdot (1 + e^{-\lambda_i \cdot D}) \quad (7)$$

to the regenerated 415 nm dose curves and applying all aforementioned aspects of $\text{Al}_2\text{O}_3:\text{C}$ radiofluorescence probe dosimetry, the dose rates for the 10 ^{137}Cs sources of the RL instrument are $\dot{D}_1=(4.86\pm 0.15)$ Gy h^{-1} , $\dot{D}_2=(4.80\pm 0.18)$ Gy h^{-1} , $\dot{D}_3=(4.11\pm 0.11)$ Gy h^{-1} , $\dot{D}_4=(4.07\pm 0.11)$ Gy h^{-1} , $\dot{D}_5=(3.86\pm 0.07)$ Gy h^{-1} , $\dot{D}_6=(3.60\pm 0.14)$ Gy h^{-1} , $\dot{D}_7=(3.74\pm 0.09)$ Gy h^{-1} , $\dot{D}_8=(3.64\pm 0.10)$ Gy h^{-1} , $\dot{D}_9=(3.76\pm 0.10)$ Gy h^{-1} and $\dot{D}_{10}=(4.61\pm 0.13)$ Gy h^{-1} in terms of a feldspar dose (error at 95% confidence level, date of calibration: 03/21/2002).

These results and the dosimetric considerations above should encourage others to use this material also for TL and OSL calibrations as a standard dosimeter. Dating results of all luminescence dating laboratories world-wide could then be straightforward and comparable. A German standard calibration protocol for β sources applied to luminescence dating following mentioned dosimetric aspects is being prepared.

4 Infrared radiofluorescence (IR-RF) dating

In the pioneering IR-RF dating work by Trautmann and Trautmann et al. (37; 11), the method was applied to different Quaternary sediment samples and showed good agreement with independent ages (^{14}C) or other luminescence dating methods and geological settings. Since then, a large number of Quaternary sediment samples has been successfully dated. As an example, in this paper we report on dating results of three samples from Quaternary sequences in Switzerland (GOS4) and Germany (HURL1, KOE10a) (see section 2.4 for a sample description). We discuss RF spectra of the samples, fit data and evaluate the physical liability of the dating results using IR-RF. Estimated IR-RF ages and the comparison with independent and other luminescence ages are presented in table 1.

4.1 RF spectra

The natural spectra in figure 4 show the influence of the spread of defect structures in natural grown minerals. The IR emission is the strongest of all RF bands of K-feldspar. KOE10A shows the strongest IR intensity compared to GOS4 and HURL1. Sample KOE10A underwent additional flotation to extract the whole feldspar fraction before the K-feldspars and plagioclases were separated by density. This may explain an enhanced enrichment of K-feldspars in the sample KOE10A. As a consequence, the IR emission is stronger than that of samples which were not treated by feldspar flotation. Furthermore, one can see typical feldspar emissions (see Krbetschek et al. (52)) at 290 nm, 330 nm, 415 nm, 560 nm and 710 nm and their differing intensities.

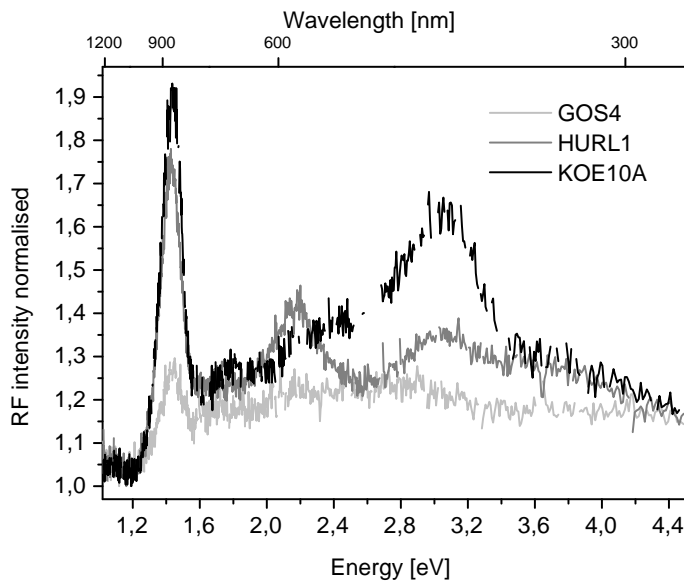


Fig. 4. Natural RF spectra (normalised) of sample GOS4, HURL1 and KOE10A with typical emission bands at 290 nm, 330 nm, 415 nm, 560 nm, 710 nm and 865 nm

The RF spectra are a good aid in recognising samples for which dating problems may occur. The complex structure of feldspar results in individually crystalline structures. Figure 5 shows the RF spectra of three bleached K-feldspar samples investigated by Dütsch (33). The mineralogical composition can be seen in the figure.

The most intensive IR-RF emission is shown in a 100% orthoclase sample (K7). The K-Na mixtures (K6, K9) exhibit a much more complex spectral situation. This implies that not only the defect inventory but also the crystalline

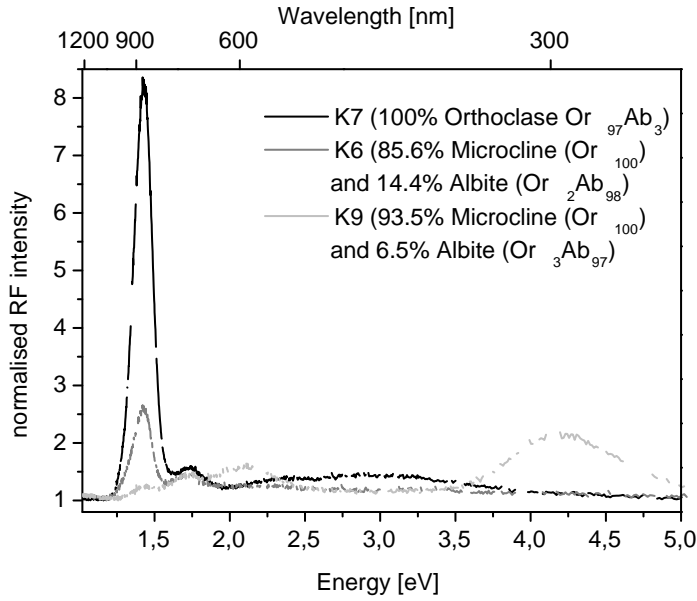


Fig. 5. Bleached RF spectra (normalised) of K-feldspar samples K7, K6 and K9 (characterised by Dütsch (33)) and their non-uniformity of qualitative and quantitative spectral RF behaviour

structure of K-feldspars does have an influence on their RF characteristics. As mentioned in section 1, in recording the RF one measures a transient equilibrium of all charge transitions in the irradiated medium. If unstable energy levels exist, this may affect the IR-RF dose record. With present day knowledge, one should especially turn attention to the red emission at 710 nm (1.74 eV) occurring in all alkali feldspars (53), because its unstable dosimetric RF behaviour could be the reason for problems connected to IR-RF dating.

4.2 IR-RF palaeodose reconstruction

The dose reconstruction was carried out on five aliquots for each sediment sample applying the IR-RF single-aliquot regenerative-dose (IRSAR) protocol after Erfurt and Krbetschek (22):

- Measurement of the natural IR-RF signal (D_{nat})
- Bleaching of the signal by a solar simulator
- Regeneration of the natural IR-RF signal (D_{nat}) using the β sources (known dose rate)
- Fitting to a stretched single-exponential decay function
- Calculation of the palaeodose (D_e)

Figures 6, 7 and 8 show the regenerative IR-RF dose curve of an aliquot of the samples GOS4, HURL1 and KOE10A. These curves are shown together with palaeodose estimation from the IR-RF dose characteristics. Note that the dose curves of samples GOS4 and KOE10A consist of 350 dose points and that of HURL1 of 200 dose points.

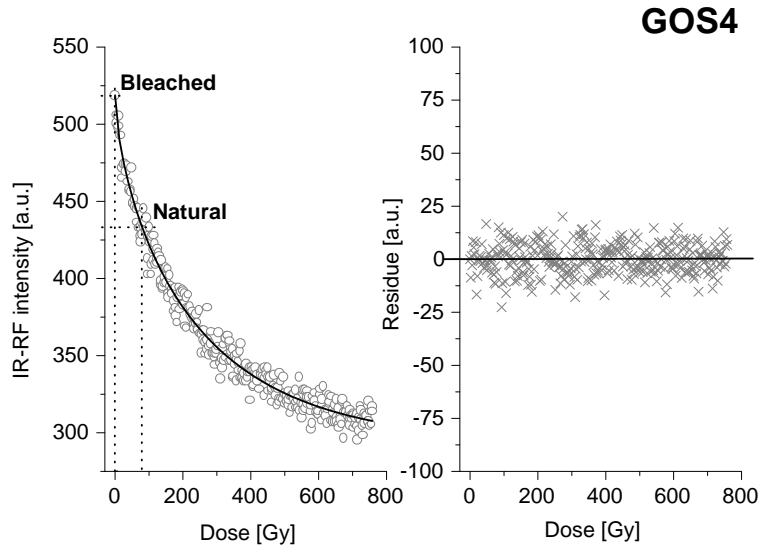


Fig. 6. Left: IR-RF dose characteristic of the 865 nm peak of sample GOS4. The data (open circles) were fitted to a stretched single-exponential function (black straight line). Right: Linear regression (straight black line) of the fit residues (cross)

The IR-RF data were fitted to a stretched single-exponential function (equation 8)

$$\Phi(D) = \Phi_0 - \Delta\Phi \cdot (1 - e^{-\lambda \cdot D})^\beta \quad (8)$$

as recently described by Erfurt and Krbetschek (16; 22). Such a stretched exponential function can describe a behavior which is often encountered in disordered condensed-matter systems (54). The dispersion of charge carrier transition or release rates and trap energies in multiple trapping-detrapping mechanisms can be expressed by the factor β in equation 8. The factor β can be understood as a material parameter of each analysed feldspar sample. The linear regression of the fit residues in figures 6, 7 and 8 show very good agreement with the fit data. This fit function does not have influence on the model for the IR-RF kinetics, described by Trautmann (12). Palaeodoses are calculated using equation 8 together with fit parameters of the IR-RF dose curves.

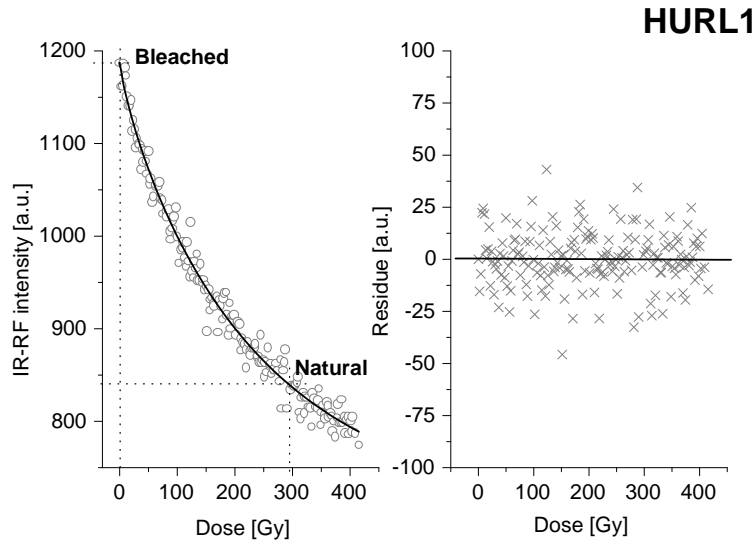


Fig. 7. Left: IR-RF dose characteristic of the 865 nm peak of sample HURL1. The data (open circles) were fitted to a stretched single-exponential function (black straight line). Right: Linear regression (straight black line) of the fit residues (cross)

Regarding all the IR-RF dose curves one can see differences in the signal dynamics and age dependency. The youngest sample (GOS4) shows the lowest dynamics which implies that younger samples may be expected to have greater scattering of palaeodose estimation results. Because this also depends on the intensity of the IR-RF signal and therefore on the PMT counting statistics this can, however, not be generalised.

Table 1

IR-RF ages, independent and other luminescence ages of the samples GOS4, HURL1 and KOE10A

Sample ID	IR-RF [ka]	^{14}C [ka]	IR-OSL [ka]	U/Th [ka]
GOS4	32.9 ± 3.4	≈ 32.0 (25)	29.5 ± 3.8 (27)	34.7 ± 4.0 (26)
HURL1	125.9 ± 12.2	-	134.8 ± 11.6	120.3 ± 5.8 (31)
KOE10A	164.4 ± 15.6	-	-	-

The age of sample GOS4 is reasonably well established by ^{14}C , U/Th, and IR-OSL dating (see table 1) (25; 26; 27; 28). HURL1 was taken from sediments of expected last interglacial age that has been confirmed by U/Th dating (31). In comparison to the cited ages of sample GOS4 ($D_e = (77.94 \pm 5.94)$ Gy) and HURL1 ($D_e = (295.73 \pm 15.79)$ Gy), determined by ^{14}C , U/Th and the IR-OSL method on feldspar, the estimated IR-RF ages show very good agreement. For sample KOE10A age control is restricted to the correlation with the Saalian

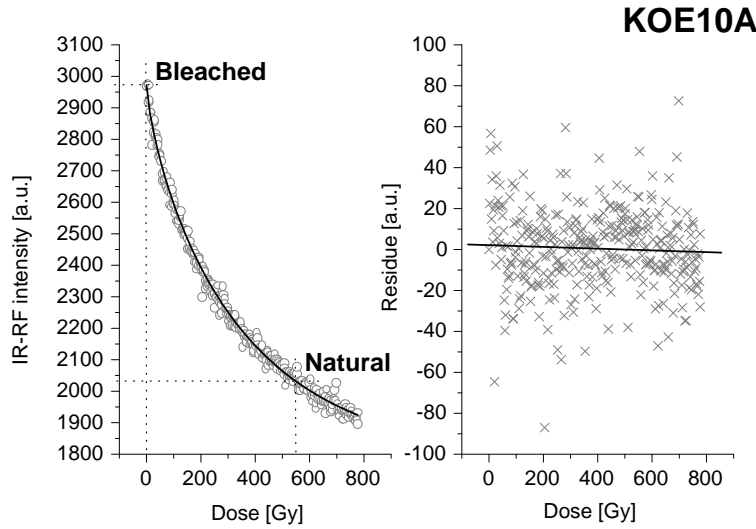


Fig. 8. Left: IR-RF dose characteristic of the 865 nm peak of sample KOE10A. The data (open circles) were fitted to a stretched single-exponential function (black straight line). Right: Linear regression (straight black line) of the fit residues (crosses)

complex that is older than the last (Eemian) interglacial. The expected age of this sample is thus between 150..220 ka. The IR-RF age of sample KOE10A ($D_e=(547.91\pm 16.15)$ Gy) does agree with this assumption. Furthermore, from a physical point of view the model of Trautmann (12) and its verification as well as the introduction of the stretched exponential decay function by Erfurt and Krbetschek (16), leave no doubt about the validity of the physical background and thus of the basic correctness of the data of older samples without independent age control. The upper detection limit (dating limit) is connected with insufficient IR-RF dose resolution, if the palaeodose is close to the saturation level of IR-RF dose function. Trautmann et al. and Erfurt and Krbetschek (11; 22) found a high thermal stability (up to 250°C) of the IR-RF signal, therefore the general reliability of the IR-RF method for the age determination of sediments of up to 250 ka may be concluded from this physical behaviour and the mean IR-RF saturation dose. However, the saturation dose and the thermal behavior of the IR-RF of K-feldspar do have the potential to increase the age upper limit. That requires further investigation, in particular the analysis of all optical RF charge transitions, in order to use RF signals connected to thermal instabilities or those connected to tunneling effects which affect the transient equilibrium of the IR-RF method (16).

4.3 VIS radiofluorescence of K-feldspar

As proposed by Erfurt and Krbetschek (16), the measurement of all optical RF transitions may help to determine the influence of instabilities of charge trapping during the IR-RF and also during the IR-OSL process. This is technically possible due to the automated filter wheel we have implemented, which offers 4 positions for various optical filters. We separate all emissions using very narrow-band interference filters (Andover FC-series, FWHM about 15 nm). Figure 9 shows an example of sample SHO.

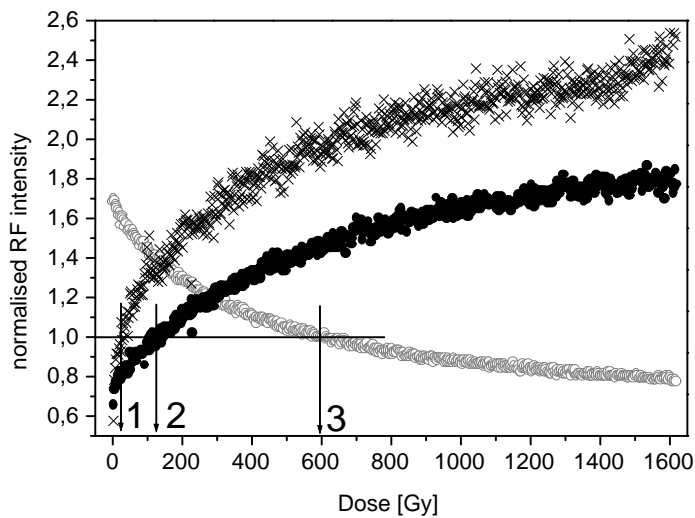


Fig. 9. Sample SHO: RF dose characteristics of the 415 nm emission (black circles), 710 nm emission (black crosses) and the IR-RF at 865 nm (open gray circles) used for dating

Beside the IR-RF, the red and blue emissions (710 nm and 415 nm) were measured, also applying the IRSAR protocol (22). The figure 9 shows the dose curves, and these records of each RF emission were normalised by the natural signals of each individual emission. Therefore, one can determine the stabilities of the different emission bands under study. Trautmann et al. (11) explained the behaviour of the red RF emission at 710 nm and its instability due to high probability of charge tunneling (\rightarrow 1 in figure 9). Regarding the dose curves of this sample in figure 9, the palaeodose determined with the IR-RF method is about 600 Gy (\rightarrow 3). The IRSAR protocol applied to the blue emission results in a palaeodose of only 120 Gy (\rightarrow 2). In a straightforward fashion, for the sample buried and naturally irradiated in the sediment, the estimated equivalent dose of 120 Gy using the blue RF indicates an insta-

bility of the signal. It is obvious that the blue emission shows a stability less than the IR-RF. Since the IR-OSL of K-feldspars uses this blue recombination luminescence for the detection of IR-excited electrons, this behaviour affects the IR-OSL palaeodose estimation and can be studied with such RF measurements. Also different saturation doses as well as different dynamic ranges of the three RF emissions are observable. The IR-RF saturation dose of sample SHO is about 1500 Gy and the dose curve follows the stretched exponential equation 8. However, with decreasing IR-RF intensity the dynamic range also decreases exponentially with given dose. In this sample, IR-RF dose curves would be usable up to about 800 Gy.

Regarding the calibration of the β sources using the 415 nm RF emission of $\text{Al}_2\text{O}_3\text{:C}$ (section 2.2) applied to the instrument described in this paper, and investigations on other luminophors by Erfurt and Krbetschek (24), the ability of the instrument to measure radiofluorescence in the VIS was clearly shown.

5 Summary

We have presented a new automated radioluminescence reading system, whose development was connected to a new solid state luminescence dating technique for the determination of the last light exposure of Quaternary sediments. This method uses an infrared radiofluorescence only appearing in potassium-rich feldspars such as microcline and orthoclase. The upper age detection limit of this IR-RF technique of 250 ka verifies its applicability to geochronometry tasks. Deriving from measurements of the IR-RF saturation dose of the feldspar dosimeters and the dynamic range of the IR-RF dose curve, there is potential to enhance the upper age detection limit, but more precise work is necessary to confirm this conclusion. The instrument was designed following the main features of the IR-RF dating protocol and consequently of the physical background of this new dating technique. For the calibration of the laboratory ^{137}Cs β sources, implemented in the system, a method using the blue RF emission at 415 nm of $\text{Al}_2\text{O}_3\text{:C}$ was described and its application resulted in a high calibration precision. The IR-RF dating, carried out on typical clastic sediment samples showed very good agreement with independent ages (^{14}Cs , U/Th, IR-OSL). The spectral variability of the system allows the measurement of RF emissions from 160 nm to 920 nm. We described the measurement of blue (415 nm) and red (710 nm) emissions in K-feldspar, and we used those dose curve records to describe the dosimetric potential for investigating the luminescence behaviour of K-feldspars applied to luminescence dating.

Acknowledgements

This research work would never have been possible without the precise work of Dieter Emmrich and Heidrun Püschel from the mechanical workshop of the Faculty of Chemistry and Physics of the Freiberg University of Mining and Technology. We also like to thank Dr. Rainer Pintaske from STEP Sensortechnik Pockau GmbH for the precise γ irradiations. This research work is financed by the German Ministry of Education, Research and Technology (BMBF).

References

- [1] E. Rutherford, The scattering of α and β particles by matter and the structure of the atom, *Phil. Mag.* 21 (1911) 669–688.
- [2] A. S. Marfunin, *Physics of Minerals and Inorganic Materials*, Springer, Berlin, 1979.
- [3] A. Morono, E. R. Hodgson, Radiation induced optical absorption and radioluminescence in electron irradiated SiO_2 , *J. Lum.* 72–74 (1998) 778–780.
- [4] A. Morono, E. R. Hodgson, On the origin of the F^+ centre radioluminescence in sapphire, *J. Nucl. Mat.* 249 (1997) 128–132.
- [5] T. Schilles, N. R. J. Poolton, E. Bulur, L. Bøtter-Jensen, A. S. Murray, G. M. Smith, P. C. Riedi, G. A. Wagner, A multi-spectroscopic study of luminescence sensitivity changes in natural quartz induced by high-temperature annealing, *J. of Phys. D: Appl. Phys.* 34 (5) (2001) 722–731.
- [6] R. Chen, S. W. S. McKeever, *Theory of Thermoluminescence and Related Phenomena*, World Scientific Publishing Co. Pte. Ltd, London, 1997.
- [7] Y. A. Marazuev, A. B. Brik, V. Y. Degoda, Radioluminescent dosimetry of α -quartz, *Radiat. Meas.* 24 (1995) 565–569.
- [8] A. Petö, A. Kelemen, Radioluminescence of LiF:Mg,Ti induced by 4 MeV electrons, *Radiat. Meas.* 24 (1995) 571–573.
- [9] A. Petö, A. Kelemen, Radioluminescence properties of α - Al_2O_3 TL dosimeters, *Radiat. Prot. Dos.* 65 (1996) 139–142.
- [10] T. Trautmann, M. R. Krbetschek, A. Dietrich, W. Stolz, Investigations of feldspar radioluminescence: potential for a new dating technique, *Radiat. Meas.* 29 (1998) 421–425.
- [11] T. Trautmann, M. R. Krbetschek, A. Dietrich, W. Stolz, Feldspar radioluminescence: a new dating method and its physical background, *J. Lum.* 45 (1999) 45–58.
- [12] T. Trautmann, A study of radioluminescence kinetics of natural feldspar dosimeters: experiments and simulations, *J. Phys. D: Appl. Phys.* 33 (2000) 2304–2310.

- [13] M. J. Aitken, Thermoluminescence Dating, Academic Press, London, 1985.
- [14] A. G. Wintle, Luminescence dating: Laboratory procedures and protocols, *Radiat. Meas.* 27 (1997) 769–817.
- [15] M. J. Aitken, An Introduction to Optical Dating, Oxford University Press, Oxford, 1998.
- [16] G. Erfurt, M. R. Krbetschek, Studies on the physics of the infrared radioluminescence of potassic feldspar and on the methodology of its application to sediment dating, *Radiat. Meas.* (submitted) .
- [17] N. R. J. Poolton, E. Bulur, J. Wallinga, L. Bøtter-Jensen, A. S. Murray, F. Willumsen, An automated system for the analysis of variable temperature radioluminescence, *Nucl. Instr. Meth. Phys. Res. B* 179 (2001) 575–584.
- [18] U. Rieser, M. R. Krbetschek, W. Stolz, CCD camera based high sensitivity TL/OSL spectrometer, *Radiat. Meas.* 23 (1994) 523–528.
- [19] L. Bøtter-Jensen, Luminescence techniques: Instrumentation and methods, *Radiat. Meas.* 27 (1997) 749–768.
- [20] M. R. Krbetschek, T. Trautmann, A. Dietrich, W. Stolz, Radioluminescence dating of sediments: Methodological aspects, *Radiat. Meas.* 32 (2000) 493–498.
- [21] Daybreak, TL/OSL reader - Product literature (1999).
- [22] G. Erfurt, M. R. Krbetschek, IRSAR - A single-aliquot regenerative-dose dating protocol applied to the infrared radiofluorescence (IR-RF) of coarse-grain K feldspar, *Ancient TL* (submitted) .
- [23] Hamamatsu, Photomultiplier Tubes, Hamamatsu Photonics, 1998.
- [24] G. Erfurt, M. R. Krbetschek, A radioluminescence study of spectral and dose characteristics of common luminophors, *Radiat. Prot. Dos.* 100 (2002) 403–406.
- [25] C. Schlüchter, M. Maisch, J. Suter, P. Fitze, W. A. Keller, C. A. Burga, E. Wynistorf, Das Schieferkohlenprofil von Gossau (Kanton Zürich) und seine stratigraphische Stellung innerhalb der letzten Eiszeit, *Viertelj. Schr. Nat. Forsch. Ges. Zürich* 132 (1987) 135–174.
- [26] M. A. Geyh, C. Schlüchter, Calibration of the ^{14}C time scale beyond 22,000 BP., *Radiocarbon* 40 (1998) 475–482.
- [27] F. Preusser, Luminescence dating of fluvial sediments and overbank deposits from Gossau, Switzerland fine grain dating, *Quaternary Geochronology* 18 (1999) 217–222.
- [28] F. Preusser, M. A. Geyh, M. Jost-Stauffer, C. Schlüchter, Timing of Upper Pleistocene climate change in lowland Switzerland, *Quat. Sci. Rev.* (accepted for publication) .
- [29] F. C. Bassinot, L. D. Labeyrie, E. Vincent, X. Quidelleur, N. J. Shackleton, Y. Lancelot, The astronomical theory of climate and the age of the brunhes-matuyama magnetic reversal, *Earth Planet. Sci. Letters* 126 (1994) 91–108.
- [30] J. Kovanda, Fossile Mollusken in Kalksinterbildungen (Dauchen) am am

- Lech-Ufer östlich Hurlach (nördlich Landsberg/Lech), Eiszeitalter und Gegenwart 39 (1989) 33–41.
- [31] H. Jerz, J. Mangelsdorf, Die interglazialen Kalksinterbildungen bei Hurlach nördlich Landsberg am Lech, Eiszeitalter und Gegenwart 39 (1989) 29–32.
- [32] H. Thieme, Lower Paleolithic hunting spears from Germany, *Nature* 385 (1997) 807.
- [33] C. Dütsch, Studienarbeit: Lumineszenzuntersuchungen an ausgewählten Feldspäten des Systems Or-Ab, TU Bergakademie Freiberg (1994).
- [34] G. Hütt, J. Jaek, The validity of the laboratory reconstruction of paleodose, *Ancient TL* 7 (1989) 23–26.
- [35] D. W. Zimmerman, Thermoluminescence dating using fine grains from pottery, *Archaeometry* 13 (1971) 29–52.
- [36] H. Y. Göksu, I. K. Bailiff, L. Bøtter-Jensen, L. Brodski, G. Hütt, D. Stoneham, Interlaboratory beta source calibration using TL and OSL on natural quartz, *J. Nucl. Mat.* 249 (1997) 128–132.
- [37] T. Trautmann, Radiolumineszenzuntersuchungen an Feldspat, Ph.D. thesis, Technische Universität Bergakademie, Freiberg (April 1999).
- [38] M. S. Akselrod, V. S. Kortov, D. J. Kravetsky, V. I. Gotlib, Highly sensitive thermoluminescent anion-defective α - $\text{Al}_2\text{O}_3\text{:C}$ singly crystal detectors, *Radiat. Prot. Dos.* 32 (1990) 15–20.
- [39] G. Erfurt, M. R. Krbetschek, T. Trautmann, W. Stolz, Radioluminescence (RL) behaviour of $\text{Al}_2\text{O}_3\text{:C}$ - potential for dosimetric applications, *Radiat. Meas.* 32 (2000) 735–739.
- [40] G. Erfurt, M. R. Krbetschek, T. Trautmann, W. Stolz, Radioluminescence (RL) probe dosimetry using $\text{Al}_2\text{O}_3\text{:C}$ for precise calibration of beta sources applied to luminescence dating, *Radiat. Phys. Chem.* 61 (2001) 721–722.
- [41] M. S. Akselrod, V. S. Kortov, E. Gorelova, Preparation and properties of $\text{Al}_2\text{O}_3\text{:C}$, *Radiat. Prot. Dos.* 47 (1993) 159–164.
- [42] M. S. Akselrod, S. W. S. McKeever, M. Moscovitch, D. Emfietzoglou, J. S. Durham, C. G. Soares, A thin-layer $\text{Al}_2\text{O}_3\text{:C}$ beta TL detector, *Radiat. Prot. Dos.* 66 (1996) 105–110.
- [43] M. S. Akselrod, S. W. S. McKeever, A radiation dosimetry method using pulsed optically stimulated luminescence, *Radiat. Prot. Dos.* 81 (1999) 167–176.
- [44] R. Kalchgruber, α - $\text{Al}_2\text{O}_3\text{:C}$ als Dosimeter zur Bestimmung der Dosisleistung bei der Lumineszenzdatierung, Ph.D. thesis, Ruprecht-Karls-Universität, Heidelberg (2002).
- [45] W. H. Bragg, *Studies in Radioactivity*, McMillan, New York, 1912.
- [46] L. H. Gray, The absorption of penetrating radiation, *Proc. Roy. Soc. A* 122 (1929) 647–667.
- [47] L. H. Gray, An ionization method for the absolute measurement of δ -ray energy, *Proc. Roy. Soc. A* 156.
- [48] ICRU37, Stopping powers for electrons and positrons, International Com-

- mission on Radiation Units and Measurements, Bethesda, 1984.
- [49] M. J. Berger, J. H. Hubbel, XCOM: Photon cross section on a personal computer, U.S. Department of Commerce, NIST, Gaithersburg, USA, 1987.
 - [50] M. Moscovitch, R. Tawil, M. Svinkin, Light induced fading in α -Al₂O₃:C, Rad.Prot.Dos. 47 (1993) 251–253.
 - [51] L. E. Colyott, M. S. Akselrod, S. W. S. McKeever, An integrating ultra violet-B dosimeter using phototransferred thermoluminescence from α -Al₂O₂:C, Rad. Prot. Dos. 72 (1997) 87–94.
 - [52] M. R. Krbetschek, J. Götze, A. Dietrich, T. Trautmann, Spectral information from minerals relevant for luminescence dating, Radiat. Meas. 27 (1997) 695–748.
 - [53] R. J. Brooks, A. A. Finch, D. E. Hole, P. D. Townsend, W. Zheng-Long, The red to near-infrared luminescence in alkali feldspar, Contr. Min. Petrol. 143 (2002) 484–494.
 - [54] L. Pavesi, M. Ceschini, Stretched-exponential decay of the luminescence in porous silicon, Phys. Rev. B 48 (1993) 17625–17628.